

Analysis of self-thermalization dynamics in the Bose-Hubbard model by using the pseudoclassical approach

Andrey R. Kolovsky

*Kirensky Institute of Physics, 660036, Krasnoyarsk, Russia and
Siberian Federal University, 660041 Krasnoyarsk, Russia*

(Dated: February 2, 2026)

We analyze the self-thermalization dynamics of the M -site Bose-Hubbard model in terms of the single-particle density matrix that is calculated by using the pseudoclassical approach. It is shown that a weak inter-particle interaction, which suffices to convert the integrable system of non-interacting bosons into a chaotic system, has a negligible effect on the thermal density matrix given by the Bose-Einstein distribution. This opens the door for equilibration where the two coupled Bose-Hubbard systems, which are initially in different thermal states, relax to the same thermal state. When we couple these two subsystems by using a lattice of the length $L \ll M$, we numerically calculate the quasi-stationary current of Bose particles across the lattice and show that its magnitude is consistent with the solution of the master equation for the boundary driven L -site Bose-Hubbard model.

I. INTRODUCTION

The problem of self-thermalization in many-body systems of interacting particles can be traced back to the celebrated work by Fermi, Pasta, and Ulam [1], where the authors numerically studied dynamics of interacting classical phonons. As it is well-known, they did not observe thermalization which at that time came as a big surprise. It took decades to realize that thermalization requires the presence of developed chaos [2, 3] and, if it is the case, the system does thermalize [4, 5]. In quantum physics the problem of self-thermalization has been discussed since the beginning of the millennium when the main focus in the field of Quantum Chaos has shifted to the many-body systems. Nowadays the classical, quantum, and mixed quantum-classical approaches to the self-thermalization problem are an area of active theoretical [6–13], and experimental research, with the system of ultra-cold atoms in optical lattices being the most popular platform [14, 15].

In this work we study self-thermalization dynamics of the Bose-Hubbard (BH) model – one of the paradigm models for the many-body classical and quantum chaos [16–18]. In relation to this particular system some aspects of thermalization are discussed in papers [6, 10–13]. In contrast to the cited works, the new aspect is that we address not only the equipartition of populations of the individual sites but the genuine thermalization, where the system relaxes to the thermal state with well-defined values of temperature and chemical potential.

Along with the thermalization problem we also discuss the important problem of non-equilibrium statistical mechanics, namely, the stationary current of particles across the tight-binding chain connected at its edges to particle reservoirs with different chemical potentials. We approach this problem from the first principles by modeling reservoirs by finite size BH systems. It is shown, in particular, that the occurrence of the stationary current requires the chaotic dynamics of reservoirs. We calculate the current numerically and compare results with the so-

lution of the master equation for the boundary driven BH model [19].

II. THERMAL DENSITY MATRIX

The quantum Hamiltonian of the M -site BH model reads

$$\hat{\mathcal{H}} = -\frac{J}{2} \sum_{\ell=1}^M \left(\hat{a}_{\ell+1}^\dagger \hat{a}_\ell + h.c. \right) + \frac{U}{2} \sum_{\ell=1}^M \hat{n}_\ell (\hat{n}_\ell - 1), \quad (1)$$

where $\hat{n}_\ell = \hat{a}_\ell^\dagger \hat{a}_\ell$. It is parametrized by three independent parameters – the hopping matrix element J , the microscopic interaction constant U , and the mean particle density $\bar{n} = N/M$. Notice that in the case of periodic boundary condition (the BH ring, in what follows) the Hamiltonian (1) can be rewritten in terms of the operators $\hat{b}_k = M^{-1/2} \sum_\ell \exp(i2\pi k\ell/M) \hat{a}_\ell$, taking the form

$$\begin{aligned} \hat{\mathcal{H}} = & -J \sum_k \cos\left(\frac{2\pi k}{M}\right) \hat{b}_k^\dagger \hat{b}_k \\ & + \frac{U}{2L} \sum_{k_1, k_2, k_3, k_4} \hat{b}_{k_1}^\dagger \hat{b}_{k_2}^\dagger \hat{b}_{k_3} \hat{b}_{k_4} \delta(k_1 + k_2 - k_3 - k_4). \end{aligned} \quad (2)$$

These two representations of the BH Hamiltonian, which we shall refer to as the Wannier and the Bloch representations, help us to identify the two integrable limits $J = 0$, $U \neq 0$ and $U = 0$, $J \neq 0$ where the energy spectrum of the system can be calculated analytically. In the general case $J, U \neq 0$ the BH model is known to be a chaotic system with energy spectrum obeying the Wigner-Dyson distribution [16]. This result suggests that dynamics of the many-body density matrix $\mathcal{R}(t)$, which obeys the quantum Liouville equation

$$\frac{d\mathcal{R}}{dt} = -i[\hat{\mathcal{H}}, \mathcal{R}], \quad (3)$$

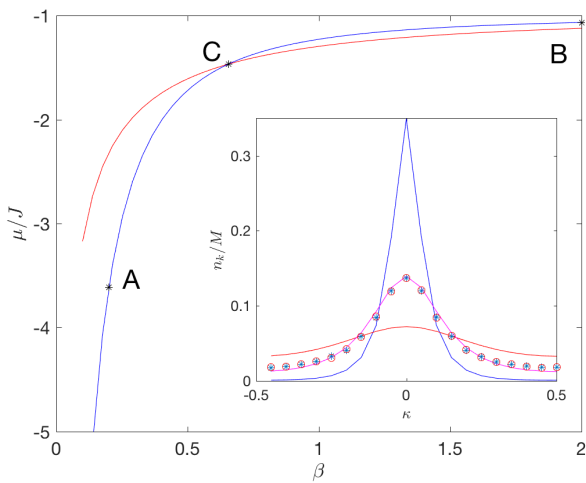


FIG. 1: Main panel: The line of constant density $\bar{n} = 1$, blue dashed curve, and the line of constant energy $\bar{E} = -0.533$, solid red curve. Inset: Bose-Einstein distributions as the function of the quasimomentum κ for the points A , C , and B , from bottom to top at $\kappa = 0$. Asterisks and open circles show the result of equilibration dynamics for two coupled rings of the size $M = 20$, see Sec. III.

should show signatures of self-thermalization. All these make the BH model a nice toy model for reviewing different aspects of statistical physics from the first principles. In particular, according to the postulates of statistical physics, the single-particle density matrix (SPDM) of weakly-interacting bosons, $\rho_{k,k'}(t) = \text{Tr}[\hat{b}_k^\dagger \hat{b}_{k'} \mathcal{R}(t)]$ should relax to the steady-state density matrix

$$\rho_{k,k'} = \delta_{k,k'} n_k, \quad n_k = \frac{1}{e^{\beta(E_k - \mu)} - 1}, \quad (4)$$

where $E_k = -J \cos(2\pi k/M)$ are energies of the single-particle eigenstates and β and μ are the inverse temperature and the chemical potential, respectively [20]. These two parameters uniquely determine the mean particle density of Bose particles in a lattice, $\bar{n} = \sum_k n_k/M$, and the mean energy per particle or lattice site, $\bar{E} = \sum_k E_k n_k/M$. The other assertion is also true, namely, the particle density \bar{n} and the mean energy \bar{E} uniquely determines the system temperature $1/\beta$ and the chemical potential μ . Notice that the latter is negative and cannot exceed $-J$, see Fig. 1.

Let us now discuss the thermal density matrix (4) from the viewpoint of the pseudoclassical approach. In what follows we prefer to work in the Wannier basis where the thermal density matrix is related to the matrix (4) by the discrete Fourier transformation.

For the finite size BH model the pseudoclassical approach is based on the notion of the Husimi function $f_{qu}(\mathbf{a}, \mathbf{a}^*; t) = \langle \mathbf{a} | \mathcal{R}(t) | \mathbf{a} \rangle$, where $|\mathbf{a}\rangle$ are the coherent $SU(L)$ states. Similar to the truncated Wigner function approach, the pseudoclassical approach amounts to approximating the governing equation for the Husimi func-

tion, which one obtains from the quantum Liouville equation (3) [21], by the classical Liouville equation

$$\frac{\partial f_{cl}}{\partial t} = \{H, f_{cl}\}, \quad f_{cl}(\mathbf{a}, \mathbf{a}^*; t=0) = f_{qu}(\mathbf{a}, \mathbf{a}^*; t=0), \quad (5)$$

where H is the classical counterpart of the quantum Hamiltonian (1),

$$H = -\frac{J}{2} \sum_{l=1}^M (a_{l+1}^* a_l + c.c.) + \frac{g}{2} \sum_{l=1}^M |a_l|^4, \quad g = U \bar{n}. \quad (6)$$

Formally, the Hamiltonian (6) follows from the quantum Hamiltonian by identifying the scaled annihilation and creation operators, $\hat{a}_\ell/\sqrt{\bar{n}}$ and $\hat{a}_\ell^\dagger/\sqrt{\bar{n}}$, with the pair of canonically conjugated variables a_ℓ and a_ℓ^* . Notice that $\sum_\ell |a_\ell|^2 = M$, which is the integral of motion of the classical BH model. The above scaling also implies the rescaled particle density $\bar{n} = 1$.

Within the framework of the pseudoclassical approach elements of the SPDM are found as

$$\rho_{\ell,\ell'}(t) = \int a_\ell^* a_{\ell'} f_{cl}(\mathbf{a}, \mathbf{a}^*; t) d\mathbf{a} d\mathbf{a}^*, \quad (7)$$

where the integral is taken over the whole phase space. Of course, solving the classical Liouville equation and calculating the multi-dimensional integral is not an easier task than solving the quantum equation of motion. Fortunately, the integral (7) can be evaluated by using the Monte-Carlo simulations. This is the main advantage of the pseudoclassical approach that we can find the SPDM without knowing the many-body density matrix $\mathcal{R}(t)$. The procedure goes as follows. It is easy to see from Eq. (4) that at $t = 0$ the classical distribution function can be sampled by the following ensemble of initial conditions

$$a_\ell = \frac{1}{\sqrt{M}} \sum_{k=1}^M \exp\left(\frac{2\pi k \ell}{M}\right) b_k, \quad b_k = \sqrt{n_k} e^{i\phi_k}, \quad (8)$$

where ϕ_k are independent random phases. In what follows we shall call this ensemble of initial conditions by the quantum ensemble. Then, evolving these trajectories in time, the elements of the SPDM Eq. (7) are calculated as

$$\rho_{\ell,\ell'} = \langle a_\ell^*(t) a_{\ell'}(t) \rangle, \quad (9)$$

where the angular brackets denote the average over the quantum ensemble of initial conditions. Notice that, although the amplitudes $a_\ell(t)$ depend on time, the average (9) does not depend on time if $g = 0$. This statement follows from the fact that for non-interacting bosons the pseudoclassical approach is exact and that for $g = 0$ the matrix (4) is a stationary state. We use this fact to control the accuracy of numerical simulations and convergence of the Monte-Carlo method. It appears that a few thousand initial conditions are sufficient to get good convergence. Further on we use 2048 trajectories.

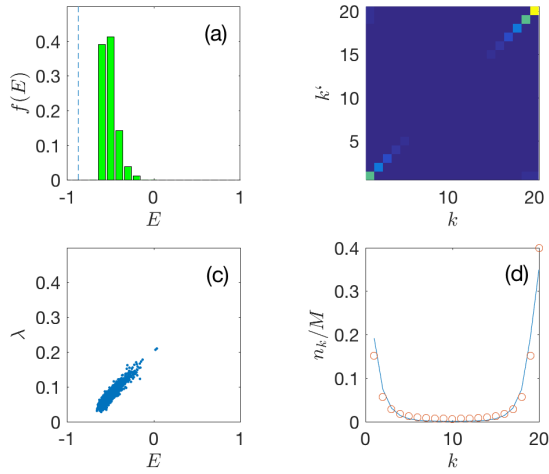


FIG. 2: Thermal density matrix for $\beta = 2$, $\bar{n} = 1$, and $g = 0.4$: (a) distribution of 2048 trajectories from the quantum ensemble over the energy; (b) the stationary SPDM in the Bloch basis; (c) Lyapunov exponents of 2048 trajectories; (d) diagonal matrix elements of the stationary SPDM, open circles, as compared to the Bose-Einstein distribution, solid line.

Is the matrix (4) a steady state in the case of weakly interacting bosons? When answering this question we focus on two cases: the low-temperature regime $\beta/J = 2$ and the high-temperature regime $\beta/J = 0.2$. In both cases the chemical potential μ is adjusted to the value ensuring the rescaled particle density $\bar{n} = 1$.

For interacting bosons we evolve trajectories according to the nonlinear equation

$$i\dot{a}_\ell = \frac{\partial H}{\partial a_\ell^*} = -\frac{J}{2} (a_{\ell+1} + a_{\ell-1}) + g|a_\ell|^2 a_\ell \quad (10)$$

and we set $J = 1$ from now on. We mention that, unlike the case $g = 0$, now different trajectories belong to different energy shells. Distribution of trajectories over the energy for $g = 0.4$ and $\beta = 2$ is depicted in Fig. 2(a), where the vertical line marks the trajectory energies for $g = 0$. Let us also mention that for $g \neq 0$ the ensemble Eq. (8) is no longer an invariant set, i.e., the classical distribution function continuously evolves in time. This, however, does not prohibit the SPDM from relaxing to a steady state. We found that in the Bloch basis this new steady state is again given by a diagonal matrix with the diagonal elements $\rho_{k,k}$ only slightly deviating from the Bose-Einstein distribution, see panels (b) and (d) in Fig. 2. The observed relaxation of the SPDM to a steady state is obviously a consequence of the coarse-graining procedure Eq. (7) and the chaotic dynamics of the system. To support the latter statement we plot in panel (c) the maximal Lyapunov exponents λ_j of all trajectories which were used to obtain results depicted in the other panels. It is seen that all trajectories from the quantum ensemble have a positive Lyapunov exponent. Moreover, the mean exponent $\bar{\lambda} \equiv \langle \lambda_j \rangle$ monotonically in-

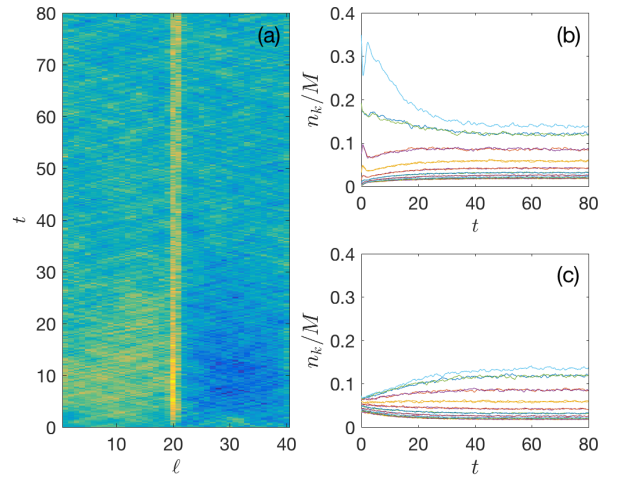


FIG. 3: Equilibration dynamics between two BH systems of the size $M = 20$ which are initially in the thermal states with $(\beta, \mu) = (2, -1.07)$ and $(\beta, \mu) = (0.2, -3.63)$, see points A and B in Fig. 1. The coupling constant $\epsilon = 0.25$.

creases with an increase of the interaction constant, see Appendix A.

In principle, a small deviation of the SPDM of interacting bosons from the Bose-Einstein distribution can be quantified, see Appendix B. In what follows, however, we shall neglect these deviations. Then the main conclusion of the present section is that the Bose-Einstein distribution, which refers to non-interacting bosons, also correctly captures the structure of the steady-state SPDM of weakly interacting bosons. However, the non-zero inter-particle interaction fundamentally changes the system dynamics, making it chaotic. In the next section we shall demonstrate that this chaotic dynamics ensures relaxation of the BH model to the thermal state for quite arbitrary initial states.

III. EQUILIBRATION DYNAMICS

Let us now consider the two BH rings which are in two different thermal states. To be specific, we shall label rings by the subindex L, the left ring, and R, the right ring. At $t = 0$ we connect them at the single site by using a reduced hopping matrix element $\epsilon < J$. Since the dynamics of every system are chaotic, it is expected that they will relax to the new thermal state which is the same for both rings.

As an example we consider the case of equal particle densities $\bar{n}_L = \bar{n}_R = 1$ but different temperatures $\beta_L = 2$ and $\beta_R = 0.2$ which corresponds to $\mu_L \approx -1.07$ and $\mu_R \approx -3.63$. Due to different temperatures the mean energies are also different, $\bar{E}_L = -0.8713$ and $\bar{E}_R = -0.1953$. When we bring the rings into contact, they can exchange particles and energy. This process is depicted in Fig. 3(a) showing populations of the lattices

sites, where the interval $1 \leq \ell \leq 20$ refer to the left ring and the interval $21 \leq \ell \leq 40$ to the right ring. Right panels in Fig. 3 show dynamics of diagonal elements of the ring SPDMs in the Bloch basis. It is seen in Fig. 3 that in the course of time rings relax to the same steady state with the SPDM diagonal elements shown by open circles and asterisks in the inset in Fig. 1. Remarkably, the latter perfectly match the Bose-Einstein distribution for $\bar{n} = 1$ and $\bar{E} = (\bar{E}_L + \bar{E}_R)/2 = -0.533$, which is depicted by the solid magenta line in Fig. 1. We would like to stress that for the considered $\epsilon = 0.25$ the discussed equilibration process involve exchange of both energy and particles. Indeed, it is seen in Fig. 3(a) that for short times hot bosons from the right ring enter the left ring, causing a temporal depletion of the right ring. Thus, during the equilibration process the two BH systems are not in the thermal states, i.e., generally do not adiabatically follow the blue line in Fig. 1 but come to the thermal state only at the end of the equilibration passage.

IV. NON-EQUILIBRIUM STEADY STATES

In this section we discuss the stationary current of Bose particles across the lattice of the length L connected at its edges to particle reservoirs with different chemical potentials. The standard approach to this problem of non-equilibrium statistical mechanics consists of two steps. First, we eliminate reservoirs and derive the master equation for the reduced density matrix $\mathcal{R}_s(t) = \text{Tr}_{L,R}[\mathcal{R}(t)]$. For example, in the Markovian case this master equation has the form

$$\frac{d\mathcal{R}_s}{dt} = -i[\hat{\mathcal{H}}_s, \mathcal{R}_s] + \sum_{i=L,R} \mathcal{L}_i(\mathcal{R}_s), \quad (11)$$

where

$$\begin{aligned} \mathcal{L}_i(\mathcal{R}_s) = & -\frac{\Gamma_i}{2} \left[(\bar{n}_i + 1) \left(\hat{a}_i^\dagger \hat{a}_i \mathcal{R}_s - 2\hat{a}_i \mathcal{R}_s \hat{a}_i^\dagger + \mathcal{R}_s \hat{a}_i^\dagger \hat{a}_i \right) \right. \\ & \left. + \bar{n}_i \left(\hat{a}_i \hat{a}_i^\dagger \mathcal{R}_s - 2\hat{a}_i^\dagger \mathcal{R}_s \hat{a}_i + \mathcal{R}_s \hat{a}_i \hat{a}_i^\dagger \right) \right] \end{aligned} \quad (12)$$

are the Lindblad relaxation operators and we use the convention $\hat{a}_{i=L} \equiv \hat{a}_1$ and $\hat{a}_{i=R} \equiv \hat{a}_L$. Next, we solve this master equation and find the stationary reduced density matrix $\mathcal{R}_s = \mathcal{R}_s(t \rightarrow \infty)$, which determines the stationary current across the chain. Remarkably, in the case of non-interacting bosons the stationary current can be found analytically [19],

$$\bar{j} = \frac{J^2 \Gamma}{J^2 + \Gamma^2} \frac{\bar{n}_L - \bar{n}_R}{2}, \quad (13)$$

where we set $\Gamma_L = \Gamma_R \equiv \Gamma$ for simplicity. The case of interacting bosons is more involved but it can be also studied, for example, by using the pseudoclassical approach [22]. The main problem of the discussed two-step approach, however, is not solving the master equation but controlling the approximations which were used to

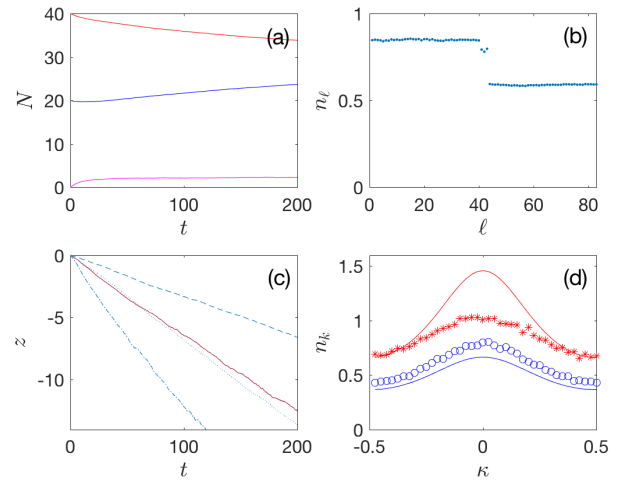


FIG. 4: Equilibration dynamics for $\epsilon = 0.1$, $M = 40$, and $L = 3$. The interaction constant for bosons in rings is $g = 0.4$ while $g = 0$ for bosons in the lattice. Initially rings are in the high-temperature thermal states with $\beta_L = \beta_R = 0.2$, and $\bar{n}_L = 1$ and $\bar{n}_R = 0.5$. Different panels shows: (a) number of particles in rings and the lattice as the function of time; (b) populations of the individual sites at $t = 200$; (c) dynamics of the quantity (14), red solid line. Additional dashed, dotted, and dash-dotted lines show $z(t)$ for $M = 20$ and $\epsilon = 0.1/\sqrt{2}$, $\epsilon = 0.1$, and $\epsilon = 0.1\sqrt{2}$; (d) diagonal elements of the ring SPDMs at $t = 0$, solid lines, and $t = 200$, markers.

derive this equation. Clearly, this is not possible without going deeper in the reservoir structure, i.e., without having a microscopic or, at least, semi-microscopic [23] model for the particle reservoir in hand. The results of the previous section suggest that the BH model suits well to our purpose.

We modify the two-ring setup of Sec. III and replace the point contact by a tight-binding chain of the length L . It is also assumed that at $t = 0$ the rings are in the high-temperature thermal states with the mean particle densities $\bar{n}_R < \bar{n}_L$. Of course, in numerical simulations we use rings of a finite size which may fully equilibrate quite rapidly. The way around this problem is to consider a small coupling constant ϵ and large M where the equilibration time is much larger than other characteristic times of the system dynamics. Then, instead of the stationary current \bar{j} we will have the quasi-stationary current $\bar{j}(t)$.

Fig. 4(a) shows dynamics of particle number in the left ring (upper line), the right ring (central line), and the lattice (lower line) for $\epsilon = 0.1$, $M = 40$, and $L = 3$. Initially the lattice is empty and the rings are in the thermal states with $\beta = 0.2$ and $\bar{n}_L = 1$ ($\mu_L \approx -3.61$) and $\bar{n}_R = 0.5$ ($\mu_R \approx -5.92$). Also we set the interaction constant g to zero for particles in the lattice. It is seen in Fig. 4(a) that after a short time required to populate the lattice we have a monotonic decrease/increase of number of particles in the left/right rings. The main result is

depicted in Fig. 4(c) by the red solid line where we plot the quantity

$$z(t) = \frac{2}{M} \log \left(\frac{\Delta N(t)}{\Delta N(0)} \right). \quad (14)$$

The linear decrease of this quantity, $z = -Ct$, indicates that the quasi-stationary current in the lattice indeed obeys the relation

$$\bar{j}(t) = C \frac{\bar{n}_L(t) - \bar{n}_R(t)}{2}, \quad \bar{n}_i(t) = \bar{n}_i(0) \mp \int_0^t \bar{j}(t') dt'. \quad (15)$$

We also depict in Fig. 4 diagonal elements of the ring SPDMs, see panel (d), and occupations of all system sites, see panel (b), where the three dots in the center refer to the lattice.

Based on numerical data in Fig. 4(c) we find the value of the relaxation constant Γ entering Eqs. (12) and (13). For $\epsilon = 0.1$ it is $\Gamma \approx 0.07$. We repeated simulations for other values of the coupling constant ϵ , see blue lines in Fig. 4(c). These simulation confirm the expected quadratic dependence of Γ on ϵ . Next, following Ref. [23] we define the self-thermalization rate of the BH model as $\gamma = \epsilon^2/\Gamma$. The obtain value $\gamma \approx 1/7$ is consistent with validity condition of the Markovian master equation (11), which requires that the self-thermalization time of particles in reservoirs has to be the shortest time scale of the problem.

V. CONCLUDING REMARKS

First of all we comment on our choice for the value of the macroscopic interaction constant $g = 0.4$. This choice is dictated by the two requirements. Namely, to use textbook statistical mechanics the interaction constant has to be as small as possible. However, to have self-thermalization we need a developed chaos that imposes the condition $g > g_{cr}$. The chosen $g = 0.4$ appears to be a good compromise between the above requirements.

The second remark concerns the self-thermalization rate γ of the BH model. We stress that we distinguish between equilibration and self-thermalization times. The former depends on the system size and typically implies that at $t = 0$ the initial state of the system strongly deviates from the thermal state. On the contrary, the self-thermalization time is independent of the system size and indicates how quickly the SPDM of the BH system comes back to the thermal states if we slight perturb this state. It is reasonable to assume that γ is determined by the mean Lyapunov exponent of the BH model which, in its turn, is determined by the value of the interaction constant g . We find that γ indeed increases as g is increased, however, the exact functional dependence of $\gamma = \gamma(g)$ remains an open problem.

This work was supported by the Russian Science Foundation under Grant No. 25-12-00268.

VI. APPENDIX A

Here we collected results of our studies on the Lyapunov exponent of the classical BH model. We calculate the Lyapunov exponent of a given trajectory by evolving the distance to its neighboring trajectory in tangential space. Fig. 5(a) shows Lyapunov exponents for $g = 0.4$, $\bar{n} = 1$, and equidistant values of the inverse temperature in the interval $0 \leq \beta \leq 2$, which correspond to different discrete values of the kinetic energy $E_K(\beta) = \sum_k E_k n_k(\beta)/M$ in the interval $-J < E_K \leq 0$. Notice that trajectories are always taken from the quantum ensemble Eq. (8). Additionally, Fig. 5(b) shows the same data yet the Lyapunov exponents are plotted as the function of the total energy $E = E_K + E_P$. It is seen, that the Lyapunov exponents grow with the trajectory energy or, what is essentially the same, with the temperature.

We also studied the dependence of λ on the interaction constant g , see Fig. 5(d), and the system size M , see Fig. 5(c), where four curves refer to $M = 10, 20, 40, 80$, from bottom to top. Notice that in Fig. 5(c) we extend the analysis onto the case of negative temperatures. Here the term ‘negative temperature’ means that the distribution function for the populations of the Bloch states is shifted by one-half of the Brillouin zone, i.e., in the limit $\beta \rightarrow -\infty$ only the Bloch state with the quasimomentum $\kappa = \pi$ is populated.

It is well-known that for $\kappa = \pi$ (in the general case, for $|\kappa| > \pi/2$) the plane-wave solution of the non-linear Schrödinger equation,

$$a_\ell(t) = \exp[i\kappa\ell + iJ \cos(\kappa)t + igt], \quad (16)$$

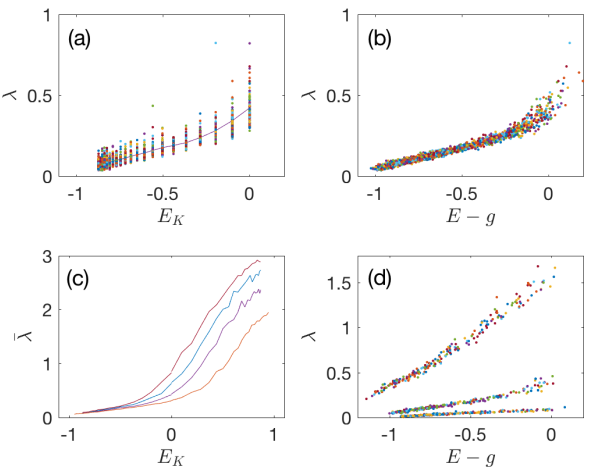


FIG. 5: (a) Lyapunov exponents for $g = 0.4$, $\bar{n} = 1$, and $M = 20$ as the function of the mean kinetic energy and (b) as the function of the total energy; (c) the mean Lyapunov exponent for $g = 0.4$, $\bar{n} = 1$, and $M = 10, 20, 40, 80$, from bottom to top, as the function of the mean kinetic energy (average over 100 initial conditions); (d) Lyapunov exponents for $\bar{n} = 1$, $M = 20$, and $g = 0.2, 0.4, 0.8$, from bottom to top, as the function of the total energy.

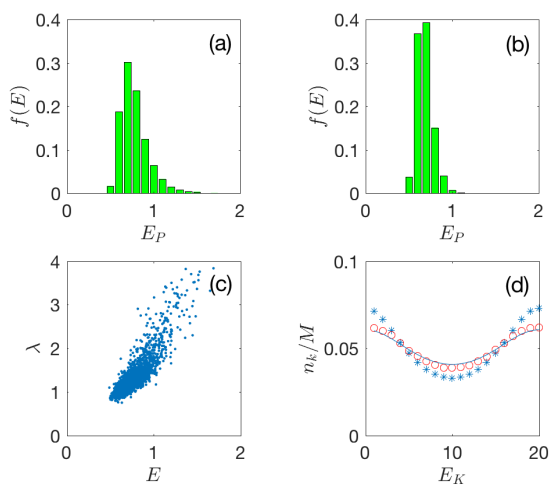


FIG. 6: Steady state SPDM for $g = 0.8$: (a)-(b) potential energy of trajectories from the quantum ensemble at $t = 0$ and t much larger than the self-thermalization time; (c) Lyapunov exponents; (d) diagonal matrix elements of the stationary SPDM, open circles, as compared to the initial Bose-Einstein distribution with $\beta = 0.2$, $\mu = -3.6125$ ($\bar{n} = 1$), asterisks, and the Bose-Einstein distribution with adjusted $\beta = 0.0980$ and $\mu = -7.1460$ ($\bar{n} = 1$), solid line.

exhibits modulation instability where the eigen-mode with $\kappa = \pi$ decay into nearby modes which, in their turn, exponentially grow in time, $|b_{\pi \pm q}(t)|^2 \sim \exp[\nu(q)t]$, with the increment [3]

$$\nu(q) = |q| \sqrt{2g/J - q^2}. \quad (17)$$

This increment gives the upper boundary for the max-

imal Lyapunov exponent. The existence of the upper boundary implies that the mean Lyapunov exponent $\bar{\lambda} = \langle \lambda(E_K) \rangle$ is finite in the thermodynamic limit $M \rightarrow \infty$. However, as it is seen Fig. 5(c), the convergence is not uniform with respect to the trajectory energy.

VII. APPENDIX B

To have a reference point we repeated calculations of Sec. II for $\beta = 0.2$, $\mu = -3.6125$ ($\bar{n} = 1$), and a twice larger value of the interaction constant $g = 0.8$, that leads to a larger deviation of the new steady-state SPDM from the Bose-Einstein distribution, see Fig. 6(d). In order to qualify this deviation, we plot in the upper panels in Fig. 6 distributions of the potential energy E_P ,

$$E_P = \frac{g}{2} \sum_{\ell=1}^M |c_\ell|^4 \quad (18)$$

for trajectories from the quantum ensemble for $t = 0$ and $t \rightarrow \infty$. These distributions give the following values for the mean potential energy per site $\bar{E}_P(0) = 0.7798$ and $\bar{E}_P(\infty) = 0.6825$. Thus, during the self-thermalization process a part of the potential energy is transformed into kinetic energy. Then, if we identify the mean kinetic energy of bosons with the temperature, the diagonal elements of the SPDM should be compared not with the Bose-Einstein distribution for $\beta = 0.2$ but with that for higher temperature which corresponds to the new kinetic energy. This distribution is depicted in Fig. 6(d) by the solid line and corresponds to $\beta = 0.0980$ and $\mu = -7.1460$ ($\bar{n} = 1$). A good agreement is noticed.

[1] E. Fermi, J. Pasta, and S. Ulam, Los Alamos Report LA-1940 (1955).

[2] F.M. Izrailev, A. I. Khisamutdinov, and B. V. Chirikov, Preprint No 252, Institute Nuclear Physics, Novosibirsk (1968).

[3] G. P. Berman and A. R. Kolovsky, *The limit of stochasticity for a one-dimensional chain of interacting oscillators*, Soviet Physics JETP **60**, 1116 (1984).

[4] G. Berman and F. Izrailev, *The Fermi-Pasta-Ulam problem: fifty years of progress*, Chaos **15**, (2005).

[5] H. Christodoulidi and S. Flach, *Measuring FPUT thermalization with Toda integrals*, Chaos **35**, 113127 (2025).

[6] A. C. Cassidy, D. Mason, V. Dunjko, and M. Olshanii, *Threshold for Chaos and Thermalization in the One-Dimensional Mean-Field Bose-Hubbard Model*, Physical Review Letters **102**, 025302 (2009).

[7] A. Polkovnikov, K. Sengupta, A. Silva, and M. Vengalattore, *Colloquium: Nonequilibrium dynamics of closed interacting quantum systems*, Reviews of Modern Physics **83**, 863 (2011).

[8] F. Borgonovi, F. M. Izrailev, L. F. Santos and V. G. Zelevinsky, *Quantum chaos and thermalization in isolated systems of interacting particles*, Physics Reports **626**, 1 (2016).

[9] A. P. Luca D'Alessio, Yariv Kafri and M. Rigol, *From quantum chaos and eigenstate thermalization to statistical mechanics and thermodynamics*, Advances in Physics **65**, 239 (2016).

[10] W. Beugeling, R. Moessner, and M. Haque, *Finite-size scaling of eigenstate thermalization*, Physical Review E **89**, 042112 (2014).

[11] T. Engl, J. Dujardin, A. Argüelles, P. Schlagheck, K. Richter, and J. D. Urbina, *Coherent backscattering in Fock space: A signature of quantum many-body interference in interacting bosonic systems*, Physical Review Letters **112**, 140403 (2014).

[12] P. Schlagheck and D. L. Shepelyansky, *Dynamical thermalization in Bose-Hubbard systems*, Physical Review E **93**, 012126 (2016).

[13] Yulong Qiao, F. Grossmann, P. Schlagheck and G. M. Lando, *Quantum Enhancement of Thermalization*, Physical Review Letters **135**, 060404 (2025).

- [14] S. Trotzky, Y. Chen, A. Flesch, I. P. McCulloch, U. Schollwöck, J. Eisert, and I. Bloch, *Probing the relaxation towards equilibrium in an isolated strongly correlated one-dimensional Bose gas*, *Nature Physics* **8**, 325 (2012).
- [15] A. M. Kaufman, M. E. Tai, A. Lukin, M. Rispoli, R. Schittko, P. M. Preiss, and M. Greiner, *Quantum thermalization through entanglement in an isolated many-body system*, *Science* **353**, 794 (2016).
- [16] A. R. Kolovsky and A. Buchleitner, *Quantum chaos in the Bose-Hubbard model*, *Europhysics Letters* **68**, 632 (2004).
- [17] A. R. Kolovsky, *Bose-Hubbard Hamiltonian: Quantum chaos approach*, *International Journal of Modern Physics B* **30**, 1630009 (2016).
- [18] L. Pausch, E. G. Carnio, A. Buchleitner and A. Rodriguez, *Chaos in the Bose-Hubbard model and random two-body Hamiltonians*, *New Journal of Physics* **23**, 123036 (2021).
- [19] A. R. Kolovsky, Z. Denis, and S. Wimberger, *Landauer-Büttiker equation for bosonic carriers*, *Phys. Rev. A* **98**, 043623 (2018).
- [20] Charles Kittel, *Thermal Physics*, 1969.
- [21] F. Trimborn, D. Witthaut, and H. J. Korsch, *Exact number-conserving phase-space dynamics of the M-site Bose-Hubbard model*, *Physical Review A* **77**, 043631 (2008).
- [22] A. A. Bychek, P. S. Muravev, D. N. Maksimov, and A. R. Kolovsky, *Open Bose-Hubbard chain: Pseudoclassical approach*, *Phys. Rev. E* **101**, 012208 (2020).
- [23] P. S. Muravev, D. N. Maksimov, and A. R. Kolovsky, *Resonant transport of bosonic carriers through a quantum device*, *Physical Review A* **105**, 013307 (2022).